Int J Adv Manuf Technol (2014) 72:1133–1141
DOI 10.1007/s00170-014-5769-8

ORIGINAL ARTICLE

Numerical simulation and experimental investigation to improve the dimensional accuracy in electric hot incremental forming of Ti–6Al–4V titanium sheet

Guoqiang Fan · L. Gao

Received: 23 August 2013 / Accepted: 6 March 2014 / Published online: 28 March 2014

Abstract Electric hot incremental forming is feasible and easy to control to form hard-to-form sheet metals, but the limited accuracy is a major deficiency. In order to find methods to improve precision, single-point electric hot incremental of Ti–6Al–4V titanium sheet was numerically simulated using MSC.Marc, and experimental investigations were also carried out in this paper. Through numerical analysis, distributing laws of temperature, thermal strain, stress, and equivalent strain were revealed, and impacts of cold contract and thermal strain on forming were also revealed. Analysis showed that electric hot incremental forming is a complex pyroplastic deformation, and there is a large internal stress in single-point electric hot incremental forming. The incremental sheet forming region can be divided into three parts: bending deformation at the beginning, shear forming at middle, and reverse bending at last; it is important to enhance the accuracy of the bending part and the reverse bending part, and adequate support must be provided in the beginning to reduce the bending part. In order to form a workpiece with small angle, two-point incremental forming was adopted at first because the gravity of clamp can reduce the reverse bending, then single-point electric hot incremental forming was adopted to enhance the accuracy and reduce internal stress of workpiece.

G. Fan (✉)
College of Mechanical and Electrical Engineering, Shandong Agricultural University, Taian 271018, People's Republic of China
e-mail: fgqnh@hotmail.com

G. Fan
Shandong Provincial Key Laboratory of Horticultural Machineries and Equipments, Taian 271018, People's Republic of China

L. Gao
College of Mechanical and Electrical Engineering, Nanjing University of Aeronautics and Astronautics, Nanjing 210016, People's Republic of China

Keywords Electric heating · Incremental forming · Numerical simulation · Ti–6Al–4V

1 Introduction

Titanium is a material extensively utilized in the aircraft industry due to the better strength-to-weight ratio compared to steel and aluminum, corrosion resistance, and high strength at elevated temperatures [1]; for example, aircraft skin, aero-engine air casings, and aero-engine by-pass duct are all made of titanium alloy sheets. Ti–6Al–4V is the most commonly used alpha/beta titanium alloy, and it accounts for approximately 80 % of the total titanium used in the USA [2]. However, the characteristics of Ti–6Al–4V, such as giant resistance of deformation, low uniform elongation, high yield-to-tensile ratio, and high springback, make cold forming difficult for Ti–6Al–4V titanium sheets, so they were generally processed by hot forming. So low-speed forming, such as superplastic forming at elevated temperature about 750~950 °C, is usually used at present [3–5]. Although superplastic forming permits the production of complex shape in sheet metal, it needs complex heat-resistant dies, expensive heating equipment, and special purpose machine. Because of high cost and long lead time, new manufacturing processes need to be optimized.

In recent years, incremental forming has emerged as a flexible forming method that allows manufacturing of 3D sculptured sheet metal parts without the need for expensive, dedicated tools [6, 7], and this process is economical to form complex parts in small to medium batches [8]. The major disadvantage of this process is that the forming time is much longer than competitive processes such as deep drawing used for mass production. Many papers are published related to the process mechanics and formability [9–12], and the limited accuracy of the single-point incremental forming process has

been identified as it is another major deficiency [6, 13]. Allwood et al. [14] report that industrial users of sheet forming processes typically specify geometric tolerances of around ±0.2 mm over the whole surface of a part, yet the performance of incremental sheet forming processes is typically more than ten times worse than this, and current incremental sheet forming processes are capable of an accuracy of only ±3 mm [14].

In order to improve the performance of the single-point incremental forming, Duflou et al. [15] employed a laser source for dynamic local heating of Al 5182, 65Cr2, and Ti–6AI–4V sheets. Experimental results demonstrate that this process variant results in reduced process forces, improved dimensional accuracy, increased formability, and reduced residual stresses. However, this process is capable of an accuracy of only ±1.5 mm, and this precision is not enough for a commercial use.

In 2008, Fan et al. [16] introduced a cheaper technique named electric hot incremental forming, based on the use of an electric current to heat the sheet metal. The technique is feasible and easy to control to form hard-to-form sheet metals like AZ31 magnesium and TiAl2Mn1.5 titanium sheets. In 2010, Fan et al. [17] used this technique to work the Ti–6AI–4V alloy demonstrating that the material can be well formed in a range of 500–600 °C. In 2012, Ambrogio et al. [1] used this technique to research the formability of lightweight alloys such as AA2024–T3, AZ31B–O, and Ti–6AI–4V. In this research, the grain distribution of the worked Ti–6AI–4V appears less organized, and the pore size decreases with the increase of temperature. According to that, the final structure of the worked Ti–6AI–4V appears with a higher density.

In 2012, Palumbo et al. [18] made an experimental investigation on the single-point incremental forming of Ti–6AI–4V component combining static heating with high tool rotation speed, and the combination of the two approaches revealed to be a feasible solution for manufacturing hard to work materials. In 2013, the use of high speed in the SPIF process was implemented by evaluating its impact on the microstructure and micro-hardness of Ti–6AI–4V by Ambrogio et al. [19] The results showed that the feed increase (and consequently the strain rate increase) does not affect the material microstructure, meaning that the supplied mechanical power is not enough to cause relevant temperature increase resulting in significant microstructure changes, also a hardness increase within 20 % was observed in the case of the Ti6Al4V alloy formed at the highest feed.

According to these studies, electric hot incremental forming maybe a good technology to form complex Ti–6Al–4V titanium sheet metal in small to medium batches, but geometric accuracy must be improved. In fact, the geometric accuracy is closely related to the stress and strain of sheet metal during the processing. In order to find the change law of stress and strain, electric hot incremental forming of Ti–6Al–4V titanium sheet was numerical analyzed with MSC.Marc in the current work, and experimental investigations were also carried out to find the method to improve the geometric accuracy.

2 Computational conditions

2.1 Finite element model

In the present paper, deformation behavior of Ti–6Al–4V titanium sheet in single-point electrical incremental forming process is numerically simulated using MSC.Marc. A pyramid with 50° wall angle (the bottom edge of 96 mm and the height of 36 mm) was simulated to be formed (see Fig. 1a). In the finite element model, a Ti–6Al–4V titanium sheet of 1-mm thickness with the side length of 100 mm × 100 mm is divided into two layers through thickness, the initial elemental dimension is 2.5 mm × 2.5 mm × 0.5 mm, and 3,200 hexahedral elements were generated. Tool's head diameter is 8 mm, and height is 34 mm, divided into 984 hexahedral elements.

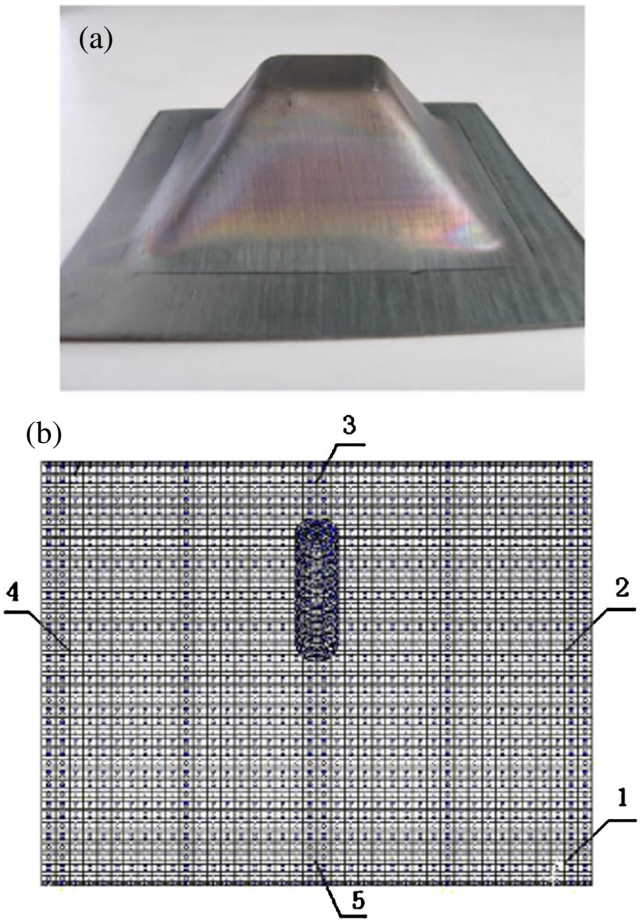

Fig. 1 Schematic showing. **a** Workpiece. **b** Numerical model of sheet

Numerical model is shown in Fig. 1b. Electricity–thermal–mechanical coupling model and hexahedral element SOLID7 was selected. Five nodes labeled in Fig. 1b were used to record analytical dates.

2.2 Physical properties of Ti–6Al–4V titanium sheet

The resistivity, conduction coefficient, specific heat, Young's modulus, and other parameters of Ti–6Al–4V alloy are shown in Tables 1 and 2 [20, 21].

2.3 Stress–strain curves of Ti–6Al–4V titanium sheet

Because Ti–6Al–4V titanium is sensitive to strain rate, and the yield stress and elongation are clearly different at different temperatures, so various stress–strain curves at different strain rates and temperatures must be used. As shown in Fig. 2, two sets of stress–strain curves were used [22]. In order to be easy inputted, the original data is simplified.

The first three layers were numerically simulated. In order to avoid complexity, the sheet mental is assumed isotropic, and heat exchange and contact resistance were neglected. In incremental forming, the forming force concentrated in tool–workpiece contact zone, and adhesion friction theory should be used [23]. After calculation, the coefficient of friction is 0.4. Current is applied to the contact area using a subroutine named flux, tool head started from node no. 1 in an anticlockwise direction, and a total of 2,440 steps were adopted.

3 Numerical simulation

3.1 Temperature change tend

Because of one-sided electric heating, the temperature of sheet mental is not uniform in 3D space, so temperatures of tool–workpiece contact side and opposite side were investigated. When the tool diameter was 6 mm, pitch was 0.2 mm, feed rate was 900 mm/min, and current was 400 A. A detailed view of the simulated temperature was shown in Fig. 3. The temperature contour of the final step was shown in Fig. 3a, and the temperature trend of the 49th step in the first layer was shown in Fig. 3b.

As can be seen from Fig. 3a, after the tool head passing, a heat conduction and diffusion track were left behind, heat gradually spread to the surrounding area, and the temperature decreased. Since the processing path of tool head is continuously superposed, the temperature field is in a comprehensive effect of diffusion and overlay. It is noteworthy that the highest temperature was in the rear of the contact area because of the integrated result of tool head movement speed and heat transfer rate of Ti–6Al–4V titanium sheet. This can be

Table 1 Material properties of Ti–6Al–4V alloy

Resistivity, ρ/(μΩ m)	1.70 (20 °C)	1.76 (100 °C)	1.82 (200 °C)	1.86 (300 °C)	1.89 (400 °C)	1.91 (500 °C)	1.92 (600 °C)	1.92 (700 °C)	1.91 (800 °C)
Conduction coefficient, λ/(W/(m c))	6.8 (20 °C)	7.4 (100 °C)	8.7 (200 °C)	9.8 (300 °C)	10.3 (400 °C)	11.8 (500 °C)	17.5 (650 °C)	23.5 (950 °C)	24.5 (1,100 °C)
Specific heat, c/(J/(Kg °C))	550 (100 °C)	590 (200 °C)	620 (400 °C)	730 (600 °C)	910 (800 °C)	950 (1,000 °C)	1,000 (1,100 °C)		
Young's modulus, E/(GPa)	67 (20 °C)	47.5 (200 °C)	39.2 (400 °C)	22.5 (600 °C)	7.45 (800 °C)	2.76 (900 °C)	8.3 (1,000 °C)	6.75 (1,100 °C)	
Other parameters	Density (ρ/(kg cm^{-3})) 4.44		Poisson's ratio (μ) 0.3		Coefficient of thermal expansion (α/(°C^{-1})) 10.5×10^{-5}		Coefficient of heat transfer (h/(kw m^{-2} K)) 20		Emissivity (ε) 0.6

Table 2 Stress of nodes on the tool–workpiece contact side and the opposite side (MPa)

No.	σ_x	σ_y	σ_z	τ_{xy}	τ_{yz}	τ_{zx}
1 (1′)	20 (−19.8)	43.4 (−183)	−53 (−1)	71.2 (−75.8)	1.4 (−16.7)	−43.8 (−51.7)
2 (2′)	243.1 (−277.7)	−348 (−247)	−74.2 (88.7)	115 (−158)	2.5 (−20.7)	−69.4 (−91.3)
3 (3′)	−129 (54)	−322 (−78)	84 (−50)	90.4 (−22.7)	−67 (−56)	−31 (−39.3)
4 (4′)	206.6 (−284.3)	−191.2 (−169)	−43 (69.6)	86.7 (−146.5)	−43.4 (−52)	−116 (−124)
5 (5′)	−59.4 (21.9)	−213.3 (48.7)	16.2 (−22.2)	27.1 (14.3)	0.25 (1.4)	−4.4 (3.5)
6 (6′)	−181.6 (65.3)	−299.4 (65.3)	98.4 (−3.5)	53.8 (18.9)	−5.1 (2.1)	30.2 (28.7)
7 (7′)	−169.2 (249)	−446.3 (134)	−145.8 (−213)	−2.9 (74.5)	63 (24.6)	−134.9 (−5.1)
8 (8′)	107.2 (−289.4)	−262.3 (−33.6)	−284.4 (−47.6)	−55.4 (−90.6)	198.3 (45.8)	134.3 (−87.5)
9 (9′)	−202.3 (−190.6)	−201.7 (−190)	−190.8 (−199.9)	−0.35 (−0.35)	4.5 (−4.1)	−3.04 (3.6)
10 (10′)	−202.3 (−190.6)	−201.7 (−190)	−190.8 (−199.9)	−0.35 (−0.35)	4.5 (−4.1)	−3.04 (3.6)
11 (11′)	−271 (−56)	−214 (−38)	−31.5 (−92)	−43 (−12)	−4.3 (53)	−28 (−31.2)
12 (12′)	20 (−317.8)	−212 (−182)	−123 (52.8)	−95 (4)	8.5 (35)	−64 (−60)
13 (13′)	−132 (−109)	−188.5 (−183)	−56 (−70)	−31.4 (26)	−13.7 (12.3)	−42.3 (−43.1)
14 (14′)	19.7 (−352)	−107 (−257)	−115 (22.9)	−101 (21.4)	−22.1 (−0.8)	−22 (−33)

confirmed in Fig. 3b. The largest temperature trend was in the rear of the contact area.

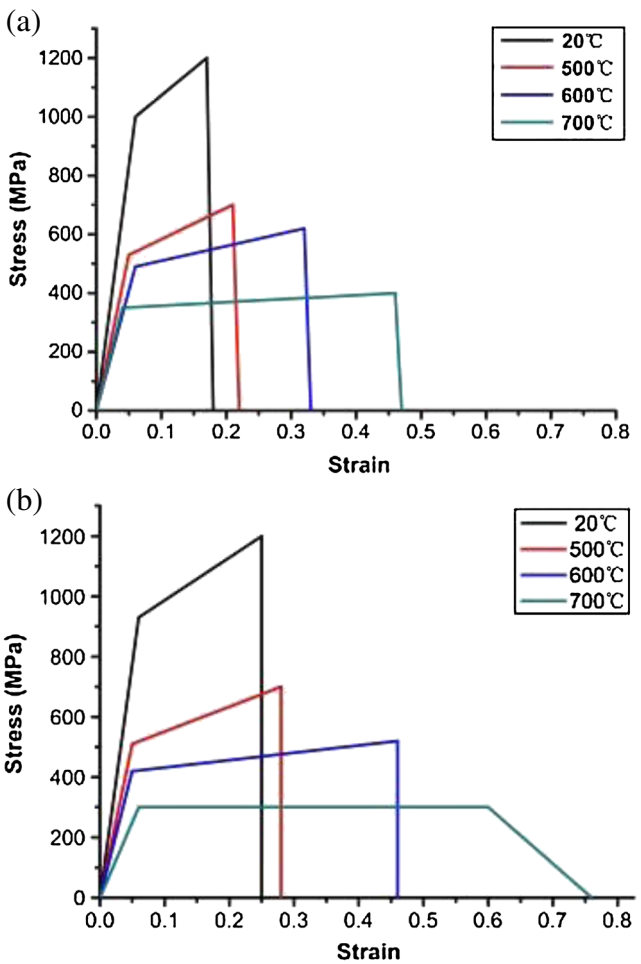

Fig. 2 Stress–strain curves of Ti–6Al–4V. **a** At 5×10^{-2} S^{-1}. **b** At 5×10^{-3} S^{-1}

The temperature change tendency of node no. 2 is shown in Fig. 4a, and it can be seen that the temperature of sheet rises rapidly by electric hot incremental forming. As the tool head passes, the temperature of sheet reaches its highest point drastically. After the tool passed, the temperature reduces slowly. As the process is carried on, the temperature gradually increases. Because of large current density and friction in the tool–workpiece contact side, the hot is mainly generated in contact side and transferred to the other side, so there is a temperature difference between both sides. That can be seen in Fig. 4b.

Based on above analysis, the temperature of the sheet mental is uneven, so the thermal stress is complex, and the dimensional accuracy will be affected.

3.2 Thermal strain

The equivalent thermal strain contours of the final step are shown in Fig. 5a, and it can be seen that, after the tool head passing, a thermal strain conduction and diffusion track was left behind, and thermal strain gradually spread to the surrounding area and decreased. With the same as temperature, the largest thermal strain was in the rear of the contact area. The thermal strain change tendency of node no. 2 is shown in Fig. 5b, and it can be seen that the thermal strain of sheet rises rapidly by electric heating. After the tool passed, the thermal stain reduces slowly.

Due to one-sided electric heating, there are two problems that must be paid attention. First, because of cold contraction, the final shape will be less than the designed shape. Second, because the thermal expansion of the contact area is larger than the other side, a stress will be given to unprocessed side by the contact side, a reverse bending of sheet will occur, and material will accumulate on both sides of the tool head. After

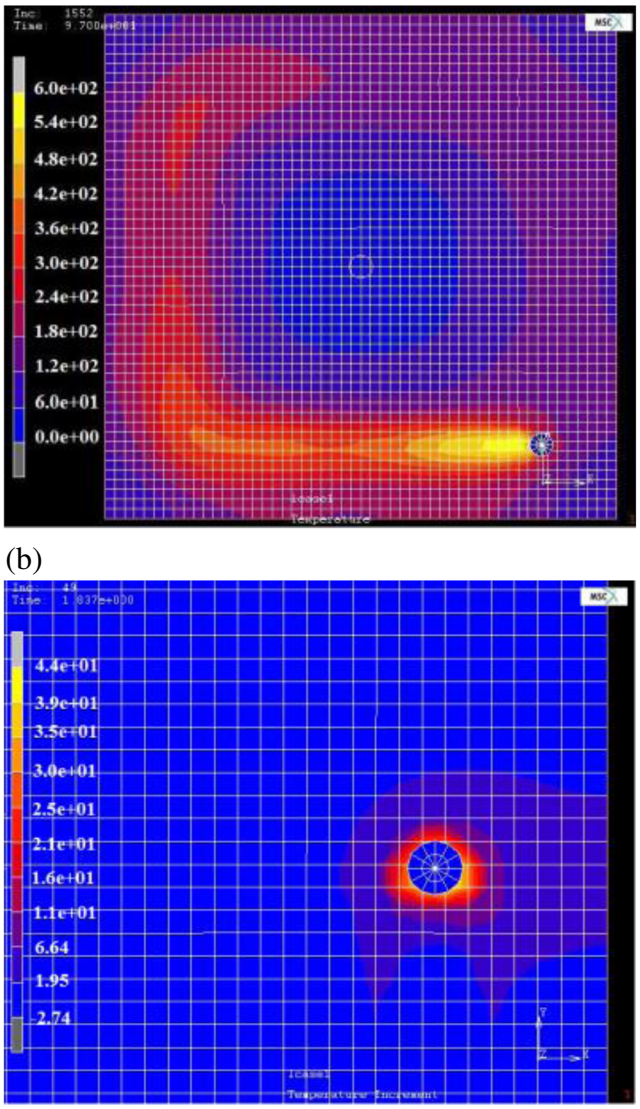

Fig. 3 Temperature change trend. **a** The temperature contour of the final step. **b** The temperature trend of the 49th step

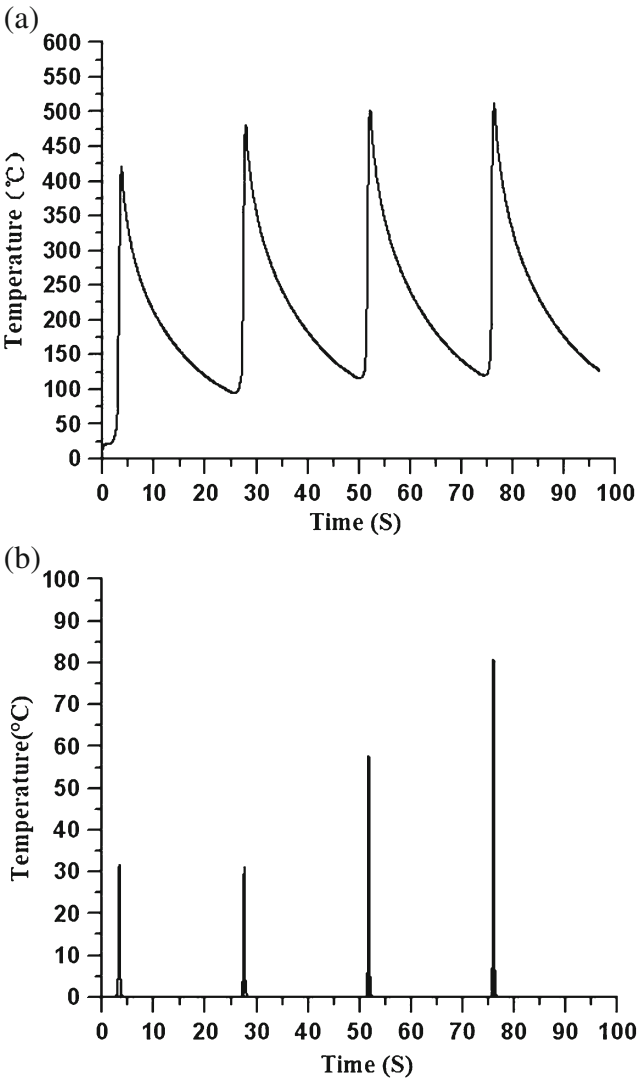

Fig. 4 Temperature change tendency. **a** Node no. 2. **b** Temperature difference between both sides

the tool passes, with the heat transfer, the temperature of contact side decreases, and the contact side of sheet cold contracts, while the other side began to expand due to thermal conduction, so a reverse bending of sheet will generate. The action of thermal strain is very similar to that of laser bending. If a workpiece with small angle is formed, the reverse bending will definitely increase with the process going on, and it can lead to processing failure.

3.3 Stress analysis

When the tool is fed to the third layer, near point no. 2, along the direction of the tool, 28 nodes on both sides of sheet were selected to study the stress in forming (as shown in Fig. 6, the right side near the pressure ring). In the analysis, nodes in contact zone with pressure ring are fixed.

Stresses of 14 points on contact side and 14 points on the other side are shown in Table 2. As can be seen from Table 2, stresses of nodes are quite complex, which include tensile stress, compress stress, and shear stress, mainly dominated by compressive stress. Stresses of nodes in the processing zone, such as nos. 3, 3′, 4, 4′, 7, 7′, 8, and 8′, are very large. Analysis showed that electric hot incremental forming is a complicated pyroplastic deformation. At the same time, stresses of node nos. 13, 13′, 14, and 14′are very large, and it can be concluded that there is a large internal stress in single-point electric hot incremental forming.

As can be seen from Table 2, node nos. 2, 4, 8, 12, and 14 are near to the blank holder; these nodes are subjected to tensile stress in the *x*-axis, while to compress stress in the *y*-

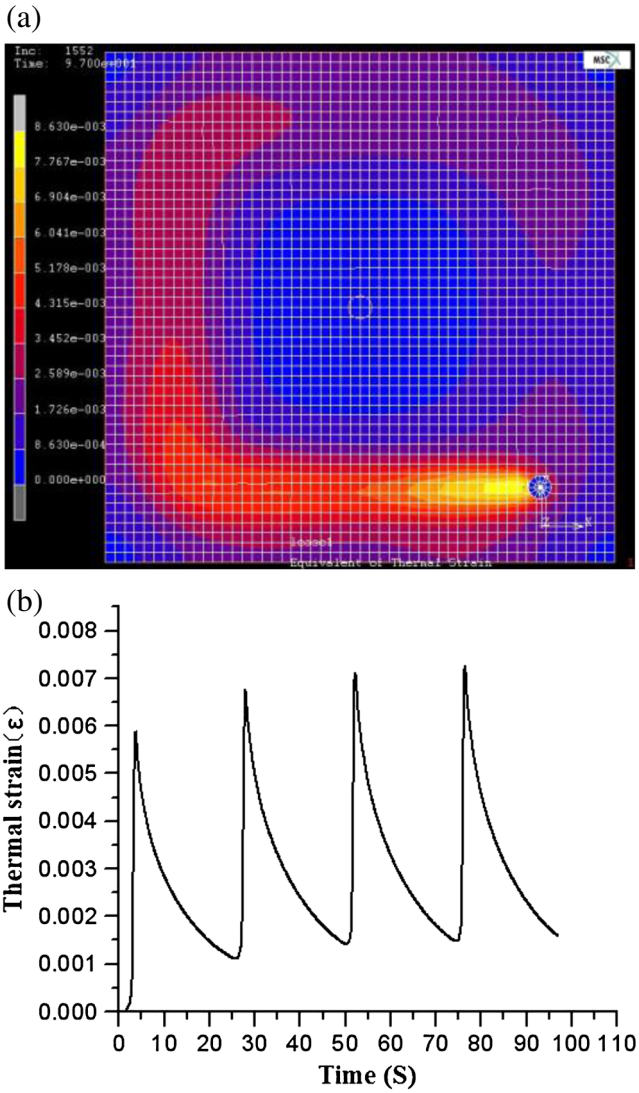

Fig. 5 Thermal strain **a** of the final step and **b** of node no. 2

axis and *z*-axis direction, the sheet on the contact side is stretched in *x*-axis direction under this condition. Stress of node nos. 2′, 4′, 8′, 12′, and 14′ is mainly compressive in the *x*-axis and *y*-axis, and the sheet on unprocessed side is compressed in *x*-axis. It can be concluded that the forming of sheet is mainly bending at the beginning (see Fig. 7), and sidewall is formed eventually.

Node nos. 3, 5, 6, 7, 11, and 13 are away from the blank holder, their stresses are mainly compressive in three directions, and the maximum stress is at node no. 7 because of pressure processing and thermal stress. As can be seen from Table 2, node nos. 5, 6, and 7 are subjected to compress stress in the *x*-axis and *y*-axis; on the contrary, node nos. 5′, 6′, and 7′ are subjected to tensile stress in the *x*-axis and *y*-axis. Because nodes on the tool–workpiece contact side are compressed and those on the opposite side are stretched, the sheet bends upwardly. On the other hand, single-sided heating also has an impact on shaping. During the heating phase, the thermal strains will be converted into plastic compressive strains; on the cooling phase, the heated titanium sheet will undergo shrinkage, leading to the development of bending of the workpiece at the tool–workpiece contact region. In the circumstances, material will accumulate on this side (see Fig. 7), and that will be confirmed by experiments. If a workpiece with small angle is formed, the reverse bending will definitely increase with the tool feeding round and round, and it will lead to a failure. In order to reduce this reverse bending, an opposing force must be applied.

Through the above discussion, the forming of sheet is mainly dominated by compressive stress, so the forming limit and hardness of Ti–6Al–4V titanium sheet can be improved. According to the analysis of nodes' stress in different regions, the incremental sheet forming region can be divided into three parts: bending deformation at the beginning, shear forming at the middle, and reverse bending at the last (see Fig. 7). In previous studies, incremental forming was simplified as shear deformation. This conclusion cannot explain why sheet metal bends in the beginning forming zone and reverse bends in the final forming zone. It is important to enhance the accuracy of the bending deformation part and the reverse bending part.

3.4 The equivalent plastic strain

The equivalent plastic strain of no. 2 is shown in Fig. 8a; there is no plastic deformation in the first two layers because of low temperature and lack of support. In the fourth layer, the equivalent plastic strain of sheet increases rapidly. So, the deformation of first few layers is important to forming accuracy, and solutions must be found.

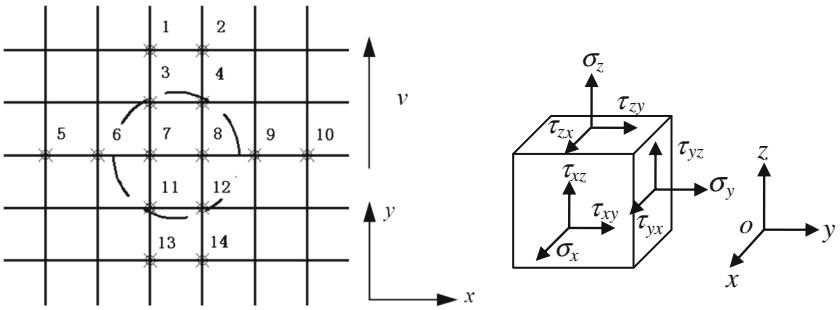

Fig. 6 The sketch of node distribution

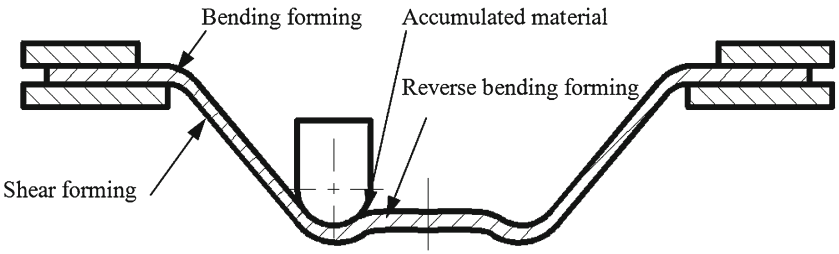

Fig. 7 The division of forming region

The equivalent plastic strain contour of the final step is shown in Fig. 8b, and it can be seen that the plastic strain near the corner is greater than those of other parts because of the support in two directions. Therefore, in order to improve the accuracy of the forming, adequate support must be provided in the beginning to reduce the bending part.

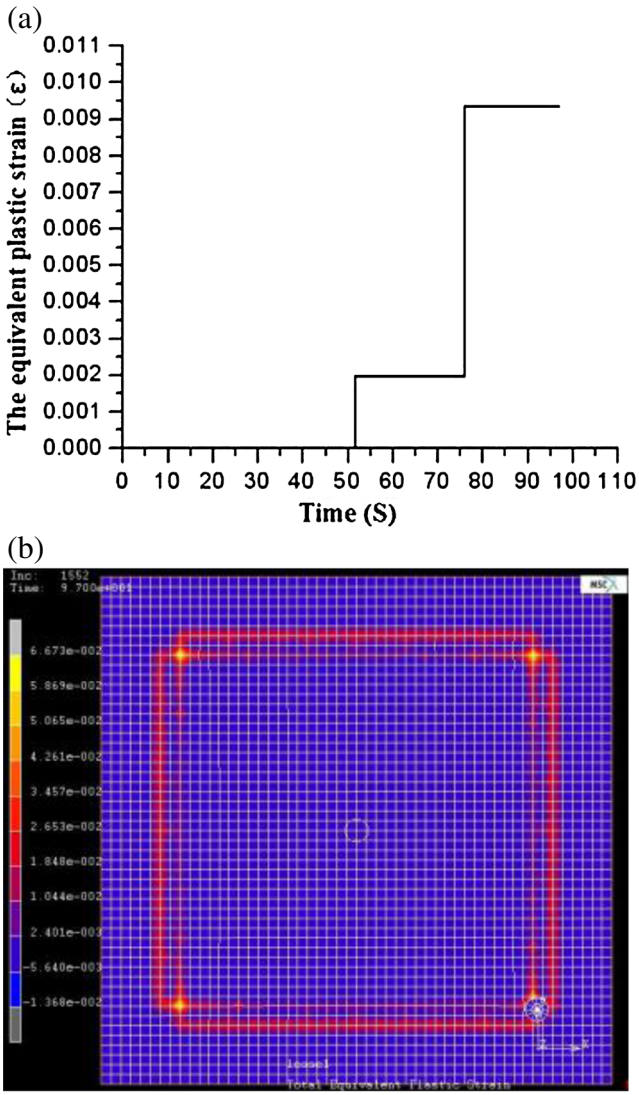

Fig. 8 The equivalent plastic strain of **a** no. 2 and **b** the final step

4 Experimental investigations

When the current was 400 A, the tool diameter was 6 mm, pitch was 0.2 mm, and feed rate was 900 mm/min, and a pyramid with 40° wall angle (the bottom edge of 96 mm and the height of 36 mm) was formed. The workpiece was cut into two halves on a wire electric discharge machine (EDM), the section plane is shown in Fig. 9, and bending deformation at the beginning, shear forming at the middle, and reverse bending at the last can be observed.

As can be seen from Fig. 9, springback occurs in the bending part due to the release of internal stress. Because of the release of internal stress, minor springback occurs in the forming wall. This is exactly the same with the numerical analysis. Adopting the same parameters, a pyramid with 30° wall angle was formed. As the process went on, a bulge occurred in the middle of the workpiece (see Fig. 10), so the forming was not successful. The result of numerical simulation was confirmed, and the solution must be found to solve the problem.

To reduce the reverse bending is important in forming workpiece with small wall angle, so two-point incremental forming was adopted because the gravity of clamp can reduce the reverse bending (see Fig. 11a). As can be seen from Fig. 11b, a pyramid with 30° wall angle was formed successfully. Because of the cold contract, the springback of forming wall occurred, so the shape of workpiece was not accurate.

In order to enhance the accuracy, the workpiece and the clamp were inversed and produced by single-point

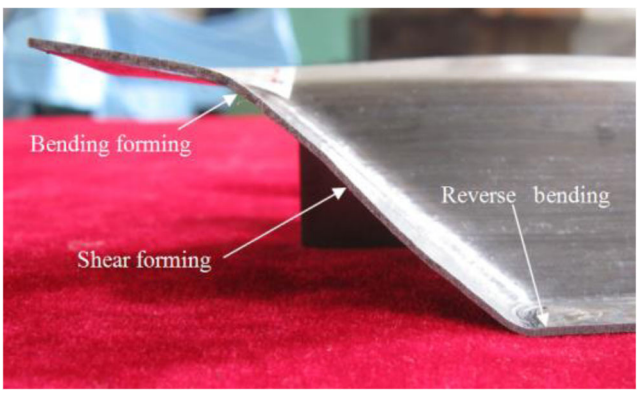

Fig. 9 Sectional shape of a workpiece

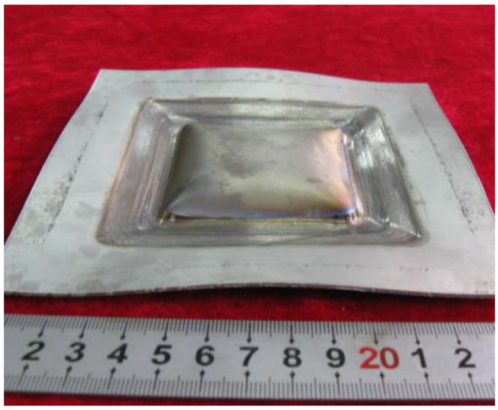

Fig. 10 A workpiece with a bulge in the middle

incremental forming. As can be seen in Fig. 12, a workpiece was formed with high accuracy. The workpiece was cut into two halves on a wire EDM machine, the section plane is shown in Fig. 12b, and the precision of forming wall is 0.3 mm. Experiments show that this technology is not only able to process workpiece with small wall angle but also improve the accuracy and reduce internal stress.

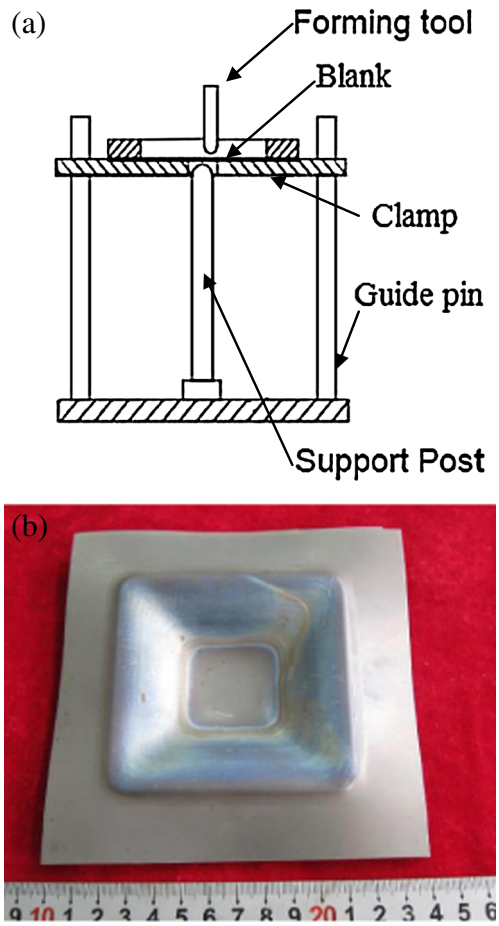

Fig. 11 **a** The sketch of two-point incremental forming. **b** A formed workpiece with small angle

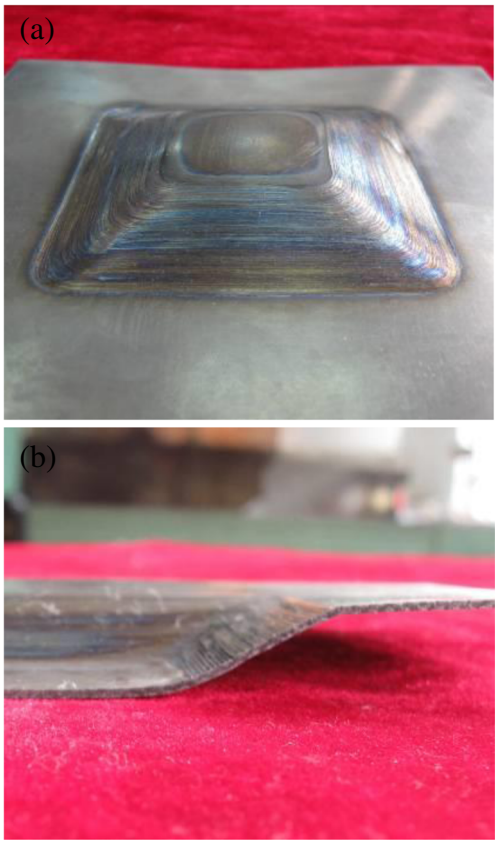

Fig. 12 A well-formed workpiece. **a** External view. **b** Sectional shape

5 Conclusions

Ti–6Al–4V is the most commonly used titanium alloy in the aerospace field. Electric hot incremental forming maybe a good technique for Ti–6Al–4V titanium sheet and has potential applications, but geometric accuracy must be improved. In order to find the method to improve the geometric accuracy, single-point electric hot incremental forming of Ti–6Al–4V titanium sheet was numerically simulated using MSC.Marc, and experimental investigations were also carried out in this study.

Experimental investigations highlighted that:

1. Through numerical analysis, distributing laws of temperature, thermal strain, stress, and equivalent strain were revealed. Because of cold contract, the final shape will be less than the designed shape. Because of thermal strain, a reverse bending of sheet will generate. Analysis showed that stresses of nodes are quite complex, which include tensile stress, compress stress, and shear stress, mainly dominated by compressive stress, so electric hot incremental forming is a complex pyroplastic deformation, and there is a large internal stress in single-point electric hot incremental forming. According to the analysis of nodes' stress in different regions, the incremental sheet forming

region can be divided into three parts: bending deformation at the beginning, shear forming at the middle, and reverse bending at the last.
2. Analysis showed that it is important to enhance the accuracy of the bending deformation part in first few layers, and adequate support must be provided in the beginning to reduce the bending part.
3. In order to form a workpiece with small angle, two-point incremental forming can be adopted at first because the gravity of clamp can reduce the reverse bending, then single-point electric hot incremental forming can be adopted to enhance the accuracy and reduce internal stress of workpiece.

Acknowledgments This study was supported by the Aviation Science Foundation of China (2008ZE52052), the Shandong Science Development Project (2013GNC11205), the Postdoctoral Sustentation Fund of Shandong Agricultural University, and the Youth Science and Technology Foundation of Shandong Agricultural University.

References

1. Ambrogio G, Filice L, Gagliardi F (2012) Formability of lightweight alloys by hot incremental sheet forming. Mater Des 34:501–508
2. Eylon D, Seagle SR (2000) In: Gorynin IV, Ushkov SS (eds) Titanium 99: science and technology. CRISM "PROMETEY", St. Petersburg, pp 37–41
3. Lee HS, Yoon JH, Park CH, Ko YG, Shin DH (2007) A study on diffusion bonding of superplastic Ti–6Al–4V ELI grade. J Mater Process Technol 187–188:526–529
4. Ghosh AK, Hamilton CH (1979) Mechanical behavior and hardening characteristics of a superplastic Ti-6A1-4V alloy. Metall Trans A 10A:699–706
5. Vanderhasten M, Rabet L, Verlinden B (2008) Ti–6Al–4V: deformation map and modelisation of tensile behaviour. Mater Des 29:1090–1098
6. Jeswiet J, Micari F, Hirt G, Bramley A, Duflou J, Allwood J (2005) Asymmetric single point incremental forming of sheet metal. Ann CIRP 54(2):623–650
7. Hussain G, Gao L, Zhang ZY (2008) Formability evaluation of a pure titanium sheet in the cold incremental forming process. Int J Adv Manuf Technol 37:920–926
8. Leach D, Green AJ, Bramley AN (2001) A new incremental forming process for small batch and prototype parts. In: Proceedings of the Ninth International Conference on Sheet Metal, Leuven
9. Kopac J, Kampus Z (2005) Incremental sheet metal forming on CNC milling machine-tool. J Mater Process Technol 162–163:622–628
10. Hussain G, Gao L, Hayat N, Dar NU (2010) The formability of annealed and pre-aged AA-2024 sheets in single-point incremental forming. Int J Adv Manuf Technol 49:543–549
11. Maria BS, Peter SN, Bay N, Martins PAF (2011) Failure mechanisms in single-point incremental forming of metals. Int J Adv Manuf Technol 56:893–903
12. Jacob S, Rajiv M, Liu WK, Jian C (2013) The formability of annealed and pre-aged AA-2024 sheets in single-point incremental forming. Int J Adv Manuf Technol 69:1185–1201
13. Hussain G, Gao L, Hayat N (2011) Forming parameters and forming defects in incremental forming of an aluminum sheet: correlation, empirical modeling, and optimization: part A. Mater Manuf Process 26(12):1546–1553
14. Allwood JM, Houghton NE, Jackson KP (2005) The design of an incremental sheet forming machine. In: Proceedings of the Shemet 2005 Conference, Erlangen, April 2005, p 471–478
15. Duflou JR, Callebaut B, Verbert J, De Baerdemaeker H (2007) Laser assisted incremental forming: formability and accuracy improvement. Ann CIRP 56:273–276
16. Fan GQ, Gao L, Hussain G, Wu ZL (2008) Electric hot incremental forming: a novel technique. Int J Mach Tools Manuf 48:1688–1692
17. Fan GQ, Sun FT, Meng XG, Gao L, Tong GQ (2010) Electric hot incremental forming of Ti-6Al-4V titanium sheet. Int J Adv Manuf Technol 49:941–947
18. Palumbo G, Brandizzi M (2012) Experimental investigations on the single point incremental forming of a titanium alloy component combining static heating with high tool rotation speed. Mater Des 40:43–51
19. Ambrogio G, Gagliardi F, Bruschi S, Filice L (2013) On the high-speed single point incremental forming of titanium alloys. CIRP Ann Manuf Technol 62:243–246
20. The editorial board of China Aeronautical Materials Handbook (2002) China aeronautical materials handbook. China Standards Press, Beijing
21. Lee RS, Lin HC (1998) Process design based on the deformation mechanism for the non-isothermal forging of Ti–6Al–4V alloy. J Mater Process Technol 79:224–235
22. Zhang HD (2006) Hot spinning process of titanium alloy collar rim of lunar rover. Dissertation, Harbin Industrial University
23. Zhao ZD, Shao MZ, Zhang ZD, Wang JA (2004) Metal forming friction and lubrication. Chemical Industry Press, Beijing